Full Length Article

Combustion and emissions characteristics of date pit methyl ester in a single cylinder direct injection diesel engine

Paul Hellier[a],[*], Farrukh Jamil[b],[d], Ernesto Zaglis-Tyraskis[a], Ala'a H. Al-Muhtaseb[b], Lamya Al Haj[c], Nicos Ladommatos[a]

[a] Department of Mechanical Engineering, University College London, Torrington Place, London WC1E 7JE, United Kingdom
[b] Department of Petroleum and Chemical Engineering, College of Engineering, Sultan Qaboos University, Muscat 123, Oman
[c] Department of Biology, College of Science, Sultan Qaboos University, Muscat 123, Oman
[d] COMSATS University Islamabad, Lahore, Pakistan

ARTICLE INFO

ABSTRACT

Current biofuels for diesel engines are largely derived from food crops and there is significant concern, recognised by legislation, that such fuels do not result in net reductions of greenhouse gas emissions when considering the entirety of the production to usage lifecycle. A potential alternative approach is to utilise the lipid content of organic waste streams arising from food crop cultivation for the manufacture of sustainable diesel fuels. This paper therefore presents experimental studies carried out on a modern direct injection diesel engine supplied with a biodiesel (fatty acid methyl esters) produced from waste date pits to determine the combustion and emissions characteristics of an alternative fuel produced from a food residue. Date pit methyl esters were tested relative to both rapeseed and soybean methyl esters, unblended and as blends with a reference fossil diesel, alongside reference fossil diesel and a commercially available fossil diesel from Oman, at constant injection timing and constant ignition timing at a constant engine speed of 1200 rpm. Gas chromatograph analysis of the methyl esters fatty acid composition found a significantly shorter mean alkyl moiety chain length and lower number of double bonds in the case of the date pit esters than either the rapeseed or soybean biodiesel. All of the methyl esters exhibited a similar duration of ignition delay less than that displayed by a reference fossil diesel, but with a higher premixed burn fraction and peak heat release rate in the case of date pit methyl esters relative to those of rapeseed and soybean. Exhaust emissions of NOx were found to be lowest for the unblended date pit methyl esters, suggesting a greater influence of adiabatic flame temperature on rates of thermal NOx production than global in-cylinder temperatures in the case of the unblended methyl esters. Relative to the reference fossil diesel and Oman diesel, all of the methyl esters tested resulted in low particulate matter emissions.

1. Introduction

Increasing acceptance as to the potentially catastrophic effects of anthropogenic climate change and the contribution of fossil fuel usage to global warming has continued to drive the identification and deployment of alternative energy sources [1–3]. Despite the increased uptake of hybrid and electric powertrains [4–6], liquid fuels are likely to remain an important energy vector within the transport sector, especially in the context of heavy duty vehicles [7]. However, recent increased recognition of the adverse health impacts of internal combustion (IC) engine exhaust species (such as NOx and PM), and in particular with regards to the levels of these emitted by diesel engines, has placed additional focus on reducing the emission of pollutants arising from combustion [8,9]. There is therefore a need for renewable fuels potentially suitable for compression ignition combustion which are sustainable in both the context of production and the exhaust emissions arising from end-usage.

While legislative targets for the percentage of transportation fuels from renewable sources have been in place for some years, for example in the EU [10], US [11] and China [12], there is now realisation that for the use of alternative fuels to result in a sustainable reduction in greenhouse gas emissions (GHG), the production of these should not compete with the cultivation of food crops. In the EU this has resulted in the limiting of the level of biofuels from food crops allowable in road transport fuels at 7%, while promoting the uptake of advanced biofuels and those from waste feedstocks which result in reduced negative

Nomenclature

DPME	date pit methyl ester	IGN	constant ignition timing
RME	rapeseed methyl ester	IMEP	indicated mean effective pressure
SME	soybean methyl ester	NOx	nitrogen oxides
SOI	start of injection	PM	particulate matter
SOC	start of combustion	CO	carbon monoxide
CAD	crank angle degrees	CO_2	carbon dioxide
BTDC	before top-dead-centre	THC	total hydrocarbons
INJ	constant injection timing	GHG	greenhouse gases
		ILUC	indirect land-use change

environmental impact through indirect land use change (ILUC) [13].

Fatty acid esters of vegetable (or animal) oils, commonly referred to as biodiesel, are the most widely utilised alternative to fossil diesel for compression ignition combustion, and the production of which in the European Union is dominated by the cultivation and use of oils from rapeseed, sunflower and, albeit to a lesser extent, soybean [14]. While the use of straight vegetable oils such as these [15,16] was given significant attention in the 1980's, several issues detrimental to engine performance were encountered, such as fuel injector coking, combustion chamber deposits, piston ring sticking, thickening and dilution of engine lubrication oil [16,17]. Transesterification of the same oils with a short chain alcohol (most commonly methanol to form fatty acid methyl esters) was found to alleviate the severity of these issues [18,19], and the identification of oils suitable for biodiesel production, and synthesis and engine testing of the resultant fatty acid esters has been the subject of many studies and review papers [19–26].

In particular, many researchers have sought to identify non-edible crops with lipid contents suitable for biodiesel production [27,28], one example of which is *Jatropha curcas L.*, a small shrub or tree the seeds of which are toxic but can contain upto approximately 50% m/m glycerides [29]. Schönborn et al. [30] tested jatropha oil methyl esters (JME) in a single cylinder diesel engine and observed ignition characteristics similar to palm methyl ester, though elevated emissions of nucleation mode particles were observed, attributed to the presence of long chain and high boiling point lignoceric methyl esters (C24:0). Similar durations of ignition delay of JME relative to PME and SME were also observed in a constant volume combustion chamber [31], and lifecycle analysis suggests that the possible reductions in global warming potential (GWP) with biodiesel production from jatropha are also comparable to that achieved with production from edible crops such as sunflower, soy and rapeseed [32,33].

A further alternative to use of oils from food crops for the production of biodiesel is the utilisation of waste edible cooking oils [34,35]. While the composition of such waste oils varies with source [36], several researchers have found these to contain elevated levels of free fatty acids (FFA) [37–39], necessitating a two-step transesterification process and resulting in reduced ester yields relative to unused oils [38]. In engine tests of waste cooking oil methyl esters relative to those from food crops, Wu et al. [40] found the waste cooking oil biodiesel to exhibit similar ignition characteristics, but a decreased reduction in particulate matter emissions relative to a fossil diesel.

The recovery of lipids suitable for biodiesel manufacture from solid waste materials and residues produced by food industries has also been considered, such as spent coffee grounds [41–43] and date pits (or seeds) [44–48]. Date palm is mostly farmed in hot arid regions, with Gulf Cooperation Council (GCC) member states the largest producers [49,50], cultivating an estimated 2.34 million tons of dates per year for human and animal consumption, up to 11.47% of which consists of pits which are not consumed or widely utilised [47]. Using various methods of solvent extraction, maximum oil yields from dried and powdered date pits of between 10.36% and 16.5 % on a dry weight basis have been reported [45,46]. Methyl ester yields of up to 85% following esterification of the extracted date pit oils have been found [47], with the physical properties of date pit biodiesel found to be broadly within the range required by legislation [46].

Chapagain et al. [44] undertook oil extractions from desert date oil kernels and esterification to both methyl and ethyl fatty acid esters. The fatty acid profile of the resultant biodiesel was found to be similar to that from soybean oil (composed primarily of fatty acids in the range C16:0 to C18:2) and tested alongside a reference fossil diesel, and a B5 blend of the two fuels, in a light-duty diesel engine. While the engine load was not maintained at a constant level for the tests, general observations of reduced NO exhaust emissions, and elevated CO levels at 1200 rpm (but reduced at 2200 rpm) of the date biodiesel blends relative to the fossil diesel were made.

Several investigations have identified relationships between the fatty acid profiles of esters from various sources of oils and the combustion performance and emissions of these biodiesels in modern diesel engines. In tests of a series of single component fatty acid methyl esters, Schönborn et al. [30] found a decrease in the duration of ignition delay with increasing fatty acid moiety alkyl chain length and degree of saturation, and found this variation in ignition delay to be the primary influence of ester molecular structure on exhaust emissions of NOx. In tests of single component fatty acid esters with rapeseed methyl ester (RME), Pinzi et al. [51] observed an increase in emissions of total hydrocarbons (THC), CO, and PM with increasing ester alkyl chain length. The increase in both CO and THC was attributed to an increase in boiling point with alkyl chain length, while it was suggested that the decrease in the relative presence of fuel bound oxygen with increasing alkyl chain length resulted in the observed higher PM emissions. Benjumea et al. [52] investigated the effects of biodiesel degree of saturation through engine tests of relatively highly saturated palm oil FAME blended with unsaturated linseed oil FAME in varying ratio. An increase in emissions of NOx with decreasing degree of saturation (increasing number of double bonds) was observed and attributed to a concurrent increase in the duration of ignition delay and the extent of the premixed burn fraction. Five single component fatty acid esters of varying carbon chain length and degree of saturation were tested as 40% v/v blends with a fossil diesel by Zhu et al. [53] at a variety of engine speed and load combinations. A decrease in the duration of ignition delay was observed with increasing ester alkyl chain length (and degree of saturation), which at high engine load resulted in an increase in emissions of HC, CO and smoke with a decrease in NOx emissions.

This paper presents the first detailed results of combustion experiments with waste date pit methyl esters (DPME) in a single-cylinder direct injection compression ignition engine, undertaken so as to investigate the combustion and emissions characteristics of a biodiesel derived from a potentially low ILUC feedstock (DPME) relative to that produced from more commonly utilised feedstocks (RME and SME). The fatty acid profile of the methyl esters was determined, with each biodiesel tested in the research engine also blended with a reference fossil diesel and compared to a fossil diesel available commercially in Oman.

2. Experimental methods

2.1. Engine and emissions testing apparatus

A modern direct injection diesel engine, converted to run as a single cylinder research engine, was utilised for all of the combustion experiments described in this work. As the date pit methyl esters under study were available in only limited quantities, use was made of a novel low volume fuel system for high pressure direct injection (sample fuel volumes of 100–250 mL at injection pressures up to 1600 bar). The engine test facility, and the experimental methodology employed, has been described in detail by the author in previous studies [54–56]. For all experiments, the low volume fuel system and sample fuel lines were held at a constant temperature of 30 ± 2.5 °C, and the engine was normally aspirated with air at atmospheric temperature and pressure throughout. Table 1 gives further specifications of the engine, while Fig. 1 displays the operating principles of the low volume fuel system in schematic form.

In addition to measurement of the in-cylinder gas pressure, for all tests the composition of the engine exhaust gas was determined with an automotive gas analyser system (Horiba MEXA9100 HEGR) and a fast particulate spectrometer (Cambustion DMS 500); the technical and measurement specification of the exhaust emissions analysers are given in Tables 2 and 3. Continuous exhaust gas sampling occurred 180 mm downstream of the exhaust valves, with sampled gas flowing through a heated line maintained at a constant temperature of 190 °C to the automotive gas analyser system. Sampling of exhaust gases for particulate measurements was also made via a heated line, with a dilution cyclone located at the connection between the engine exhaust and heated line. Exhaust gases were diluted at this point by 5:1 and were diluted a second time upon entry to the analyser by 200:1. The sample line and both dilution cyclones were heated to a constant temperature of 75 °C.

2.2. Fuels investigated

Methyl fatty acid esters of waste date pit oils, soybean oil and rapeseed oils were tested as unblended biodiesels fuels and as blends with a reference fossil diesel of zero FAME content. Date pit methyl esters (DPME) were obtained via Soxhlet extraction of lipids from dried and ground date pits and subsequent base catalysed transesterification with methanol (following separation by rotary evaporation of the extracted lipids from the solvent employed) [46], while both the soybean and rapeseed methyl esters (SME and RME respectively) were obtained from BP Global Fuels. Prior to esterification, the extracted date pit oils [46] possessed an acid value of 3.1 mg KOH/g oil, a free fatty acid content of 1.55%, a saponification value of 236 mg KOH/g oil and a density of 910 kg/m³ at 25 °C. In addition to the testing of a fossil diesel fuel with zero FAME content as a reference fuel, a commercially available diesel fuel from Oman (obtained from Oman Oil) was also tested. The Oman diesel was included in the study for interest so as to highlight the relative performance of a commercially available diesel fuel local to a potentially significant source of waste date pits for oil extraction and biodiesel production [50]. Table 4 shows the cetane and other properties of each fuel.

2.3. Determination of fatty acid composition

The fatty acid profile of each of the methyl esters tested was determined by gas chromatography with a flame ionisation detector (GC-FID), with the DPME additionally characterised by a gas chromatograph mass spectrometer (GC–MS) following production and approximately nine months ahead of engine tests (during which time the DPME was stored in an airtight vessel in the absence of light). The GC–MS (Perkin Elmer Clarus 600) analysis was undertaken with a DB-Wax column at a He carrier gas flowrate of 1.0 mL min⁻¹ and with an oven temperature range of 80 °C (held for an initial period of five minutes) to 240 °C at a ramp rate of 4 °C per minute [46]. The GC-FID (Agilent 7890b) analysis was undertaken with a SP-2380 column (30 m × 0.25, 0.20 μm), at a He carrier gas flowrate of 20 mL min⁻¹ and with an oven temperature range of 50 °C (held for an initial period of two minutes) to 250 °C at a ramp rate of 5 °C per minute. The column inlet and detector (FID) were held at temperatures of 250 °C and 260 °C respectively, and samples of DPME, RME and SME were diluted in dichloromethane to a concentration of 5000 μg/mL. Individual peaks found during analysis of these samples were identified and quantified by referencing of retention times and peak areas to those found from analysis of a 37 component FAME (Supelco) standard using the same GC-FID method. Table 5 shows the fatty acid composition of the methyl esters as determined by GC–MS and GC-FID, and the mean ester alkyl moiety carbon chain length and number of double bonds. Table 5 also shows the degree of unsaturation (DU) [58] and long chain saturation factor (LCSF) [59], calculated according to Eqs. (1) and (2) respectively from the measured fatty acid composition and methyl ester melting points (M.pt).

$$DU = (monounsaturated\ Cn:\ 1,\ wt\%) + 2(monounsaturated\ Cn:\ 2,\ wt\%)$$
$$+ 2(monounsaturated\ Cn:\ 2,\ wt\%) \tag{1}$$

$$LCSF = \sum (M.pt(K) \times Cn:\ 0,\ wt\%)/100 \tag{2}$$

2.4. Engine operating conditions

Engine tests of each FAME, reference fossil diesel, Oman diesel and blends of FAME and reference diesel were conducted at constant fuel injection timing and repeated at constant start of ignition timing. At constant injection timing, a constant start of injection (SOI) of 5 CAD BTDC was used, where SOI was taken to be the time at which the injector actuating signal commenced, while the start of combustion (SOC) for each fuel varied in accordance with the duration of ignition delay exhibited by the fuel. For constant ignition timing, the SOC (defined in CAD as the first incidence of positive apparent heat release after SOI and prior to that of peak heat release rate) always occurred at TDC by variation of the SOI, as determined by the observed ignition delay.

All tests were conducted at low load conditions at an engine speed of 1200 rpm and a fuel injection pressure of 450 bar, and to maintain a constant engine IMEP of 4.00 bar in the case of every fuel, the injection duration was varied accordingly between 624 and 686 μs. This single engine test operating condition was chosen due to the very limited availability of date pit methyl esters (~100 mL). Table 6 shows the engine and test operating conditions for each combustion experiment

Table 1
Engine specification.

|	
Engine head model	Ford Duratorq
Engine bottom end model	Ricardo Hydra
Number of cylinders	1
Cylinder bore	86 mm
Crankshaft stroke	86 mm
Swept volume	499.56 cc
Compression ratio	18.3:1
Maximum cylinder pressure	150 bar
Peak motoring pressure at test conditions	43 bar
Piston design	Central ω – bowl in piston
Oil temperature	80 ± 2.5 °C
Water temperature	80 ± 2.5 °C
Fuel injection pump	Single – cam radial – piston pump (BOSCH CP3)
High pressure fuel rail	Solenoid controlled, max. 1600 bar (BOSCH CRS2)
Injectors	6 – hole solenoid controlled (DELPHI DFI 1.3)
Electronic fuel injection system	1 μs resolution (EMTRONIX EC-GEN 500)
Shaft encoder	0.2 CAD resolution
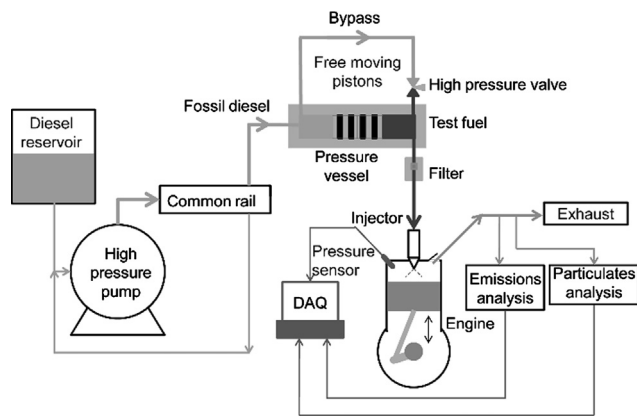
Fig. 1. Schematic showing operation of the low volume fuel system.

Table 2
Measurement specification of Horiba MEXA9100 HEGR emissions analyser.

Exhaust species	Measurement method	Accuracy
NOx	Chemiluminescence	± 0.1 ppm
CO	Non-dispersive infrared	± 0.1 ppm
CO_2	Non-dispersive infrared	± 0.1 vol/vol
O_2	Paramagnetic analysis	± 0.01 vol/vol
THC	Flame ionization detector	± 1 ppm

Table 3
Technical specification of Cambustion DMS 500 fast particulate spectrometer.

Size measurement range	5–1000 nm
No. of size classifier rings	22
Sample gas flowrate	8 L/min
Primary sample dilution ratio	5:1
Secondary sample dilution ratio	200:1

with all in-cylinder pressure data presented the average of 100 consecutive combustion cycles. The low volume fuel system and injector were flushed with the reference fossil diesel immediately after each test via the bypass shown in Fig. 1.

3. Results and discussion

3.1. In-cylinder pressure and apparent net heat release rates

Fig. 2 shows the in-cylinder pressure and apparent net heat release rates of the methyl esters, methyl ester and reference diesel blends, Oman diesel and reference diesel at both constant injection timing and constant ignition timing. At both timing conditions, higher in-cylinder pressures were produced by the reference fossil diesel than all other test fuels, while the reference fossil diesel and unblended methyl esters consistently displayed the highest and lowest rates of peak heat release respectively (Fig. 2). Also apparent in the case of the unblended methyl esters are higher levels of heat release during diffusion (or mixing rate controlled) combustion, and this is consistent with previous studies of both single component fatty acid methyl esters and biodiesels (FAME mixtures) [30,55,60]. It is also interesting to note that at constant injection timing heat release rates increase more sharply following SOC in the case of DPME than either SME or RME (Fig. 2), with the therefore suggested higher reactivity of DPME in agreement with the previously measured cetane numbers of the methyl esters (Table 4). It is tentatively suggested that this can be attributed to the low degree of unsaturation (DU) and high long chain saturation factor (LCSF) of DPME relative to RME and SME (Table 5), as while the presence of long fully

Table 4
Fuel properties.

	Cetane number	Cetane index	Density at 15 °C (kg/m³)	Kinematic viscosity at 40 °C (cST)	Initial boiling point (°C)	T50 (°C)	Final boiling point (°C)	Lower heating value (MJ/kg)	Sulphur (mg/kg)	Cloud point (°C)	H/C ratio	Oxygen content % (m/m)
Reference fossil diesel	51.7	53	834.5	2.672	179.9	268.7	356.2	43.14†	5.4	−8	1.877	0.06
Oman fossil diesel	–	56	835.7	4.10	–	–	–	–	337	−1	–	–
Date pit methyl ester [46]	58.23	54.9	870ϕ	3.97	–	–	–	41.27	0.01	4	2.257	12.00
Rapeseed methyl ester	52	57.1	883.1	4.325	312.7	335.9	354.7	–	0.1	−1	2.155	10.43
Soybean methyl ester	52	56.1	884.9	4.075	307.3	334.9	349.0	–	0.1	−1	2.075	10.82

† = calculated from experimental data obtained by the IP12 method [57].
ϕ = measured at 25 °C.

Table 5
FAME composition.

FAME	Percentage FAME composition (% m/m)										Mean alkyl moiety			
	C8:0	C10:0	C12:0	C14:0	C16:0	C16:1	C18:0	C18:1	C18:2	C18:3	Carbon chain length	No. double bonds	Degree of Unsaturation (DU)	Long Chain Saturated Factor (LCSF)
DPME (GC–MS) [46]			16.44	9.96	9.54		2.38	55.36	6.32	–	16.42	0.68	68	12.5
DPME (GC-FID)	1.5	1.5	20.1	10.4	13.6	–	2.8	32.7	7.5	1.3	15.63	0.56	54.2	16.2
RME (GC-FID)	–	–	–	–	7.6	0.6	2.3	51.7	19.7	9.1	17.82	1.31	137.2	3.3
SME (GC-FID)	–	–	–	–	13.6	–	6	21.5	41.7	10.9	17.71	1.47	159.4	6.6

saturated alkyl chains might be expected to be of most importance in determining the rates of low temperature reactions during the ignition delay period [61], it is plausible that these features of fuel molecular structure may also influence oxidation rates at the higher temperatures present following SOC [62].

3.2. Ignition delay and combustion characteristics

Fig. 3 shows the duration of ignition delay of the methyl esters, methyl ester and reference fossil diesel blends, Oman diesel and reference fossil diesel at constant injection and constant ignition timing where ignition delay is defined as the interval for each fuel between SOI and the first incidence of positive apparent heat release (SOC). In Fig. 3, and throughout this paper where error bars are given, the data point displayed is the mean value exhibited by the fuel from repeat experimental runs; the extent of the error bars are in the case of the pure reference fossil diesel plus and minus one standard deviation from this value (calculated from four repeats) and for the unblended SME the minimum and maximum values measured (from two experimental repeats). It can be seen in Fig. 3 that as the percentage FAME content of methyl ester reference fossil diesel blends increased the duration of ignition delay decreased at both timing conditions, with all of the unblended methyl esters displaying an ignition delay 0.6 CAD shorter than that of the reference fossil diesel (0% v/v FAME content) and generally consistent with the previously measured cetane numbers of the fuels (Table 4) and previous engine and constant volume chamber tests of SME [31,63] and RME [64] relative to fossil diesels. It is interesting to note, however, that at both a blend level of 20% v/v FAME and unblended, the duration of ignition delay of DPME is equivalent to, or slightly longer, than those of RME and SME (Fig. 3), despite an appreciably higher cetane number of the former (Table 4). It is tentatively suggested therefore that, at the engine operating conditions of the current study, the higher cetane number of DPME is manifest through the observed faster increase in heat release rates following SOC (Fig. 2), rather than an appreciable reduction in the duration of ignition delay [65]. Notwithstanding the engine shaft encoder resolution of 0.2 CAD, it can also be seen that the Oman diesel displayed a slightly shorter duration of ignition delay than the reference fossil diesel, but greater than that of the methyl esters (Fig. 3).

Fig. 4 shows the peak apparent net heat release rates of the methyl esters, methyl ester and reference diesel blends, Oman diesel and reference fossil diesel at both constant injection and constant ignition timing. Fig. 4 shows a linear decrease in peak heat release rates with increasing FAME content at both injection timings, with the smallest and largest decreases in peak heat release rate at an equivalent FAME content exhibited by DPME and SME respectively. The decrease in peak heat release rate with increasing FAME content, and the lower peak heat release rate of the Oman diesel relative to the reference fossil diesel (Fig. 4), can likely be attributed to a concurrent decrease in ignition delay (Fig. 3), as has previously been observed [30,54], which results in a reduced duration for fuel and air mixing prior to SOC, and thus a smaller premixed burn fraction (Fig. 2) and a more gradual release of fuel energy during diffusion combustion.

Fig. 5a and b show the calculated maximum in-cylinder global temperature and time of occurrence (as crank angle degree) of the methyl esters, methyl ester and reference diesel blends, Oman diesel and reference fossil diesel at both constant injection and constant ignition timings. Of the methyl esters, DPME and SME display the highest and lowest maximum in-cylinder temperatures respectively (Fig. 5a), in agreement with the higher peak heat release rates of DPME relative to those of SME (Fig. 4). It can also be seen that the maximum in-cylinder temperature was reached earlier in the case of unblended DPME than either RME or SME (Fig. 5b); this is especially apparent at constant injection timing and is consistent with the faster increase in heat release rates following SOC (Fig. 2) and higher cetane number (Table 4) of DPME relative to RME and SME. For all fuels tested, it can be seen that lower maximum in-cylinder temperatures were reached (Fig. 5a), and occurred later (Fig. 5b), at constant ignition timing relative to constant injection timing, and this is most apparent in the case of the unblended methyl esters, which exhibited the shortest duration of ignition delay (Fig. 3) and thus required the greatest degree of retardation of SOI to achieve SOC at TDC (Table 6).

3.3. Gaseous exhaust emissions

Fig. 6 shows the exhaust emissions of NOx of the methyl esters, methyl ester and reference diesel blends, Oman diesel and reference fossil diesel at both constant injection and constant ignition timing. Apparent in Fig. 6 is that of the unblended methyl esters, the highest and lowest levels of NOx were emitted by RME and DPME respectively at both timing conditions. It can also be seen that at constant ignition timing, that an increasing FAME content (DPME, RME and SME) resulted in a linear decrease in NOx emissions, and at both timing conditions, lower levels of NOx were emitted by the Oman diesel relative to those from the reference fossil diesel.

The production of NO_x in compression ignition engines is known to occur primarily by thermal oxidation of nitrogen, reaction rates of which increase with both increasing in-cylinder temperatures and the duration of gases at elevated temperatures sufficient for NOx formation [30,66,67]. The observed decrease in exhaust NOx emissions at constant ignition timing with increasing FAME content (Fig. 6) can therefore be attributed to both a concurrent decrease in calculated maximum in-cylinder global temperature (Fig. 5a) and a shorter duration at this temperature (Fig. 5b). However, when comparing only the unblended methyl esters, it can be seen that DPME, which emitted the lowest levels of NOx at both timing conditions (Fig. 6), exhibited both higher peak heat release rates (Fig. 4) and in-cylinder global temperatures (Fig. 5a). It is therefore tentatively suggested that the higher levels of NOx produced by both SME and RME relative to DPME might in fact be attributable to differences in adiabatic flame temperature, as has previously been observed in studies of fatty acid methyl esters where differences in fuel ignition delay have been removed through addition of the ignition improver, 2 ethylhexyl-nitrate [30]. The adiabatic flame temperatures of single component fatty acid esters increase with both increasing fatty acid alkyl chain length and degree of unsaturation [30], and so it is hypothesised that the large percentage of C12 to C16 fully saturated

Table 6
Engine and test operating conditions.

Fuel	FAME content (% wt/wt)	Engine speed (rpm)	Fuel injection pressure (bar)	IMEP (bar)	Constant injection timing, SOI at 5 CAD BTDC (INJ)				Constant ignition timing, SOC at TDC (IGN)			
					Ignition delay (CAD)		Injection duration (μs)		Ignition delay (CAD)		Injection duration (μs)	
					Mean	1 δ	Mean	1 δ	Mean	1 δ	Mean	1 δ
Reference fossil diesel	0	1200	450	4	4.6	0.0	633	5.1	4.7	0.1	633	5.3
Oman fossil diesel	0	1200	450	4	4.4	–	641	–	4.4	0.0	636	–
DPME	100	1200	450	4	4.0	–	666	–	4.0	–	666	–
SME	100	1200	450	4	4.0	0.0	680	6.5	4.0	–	685	–
RME	100	1200	450	4	4.0	–	672	–	4.0	–	674	–
SME in reference fossil diesel	10.0	1200	450	4	4.4	–	642	–	4.5	–	641	–
RME in reference fossil diesel	9.9	1200	450	4	4.4	–	642	–	4.4	–	640	–
DPME in reference fossil diesel	19.8	1200	450	4	4.4	–	638	–	4.4	–	635	–
SME in reference fossil diesel	19.9	1200	450	4	4.4	–	645	–	4.3	–	645	–
RME in reference fossil diesel	19.9	1200	450	4	4.2	–	645	–	4.3	–	640	–

esters present (and thus shorter mean alkyl moiety length and lower mean number of double bonds) in the case of DPME relative to RME and SME (Table 5) results in lower local flame temperatures and thus reduced rates of NOx formation, despite higher global temperatures (Fig. 5a) and peak heat release rates (Fig. 4) attributable to a larger premixed burn fraction (Fig. 2).

Fig. 7a and b show the exhaust CO and THC emissions of the methyl esters, methyl ester and reference diesel blends, Oman diesel and reference fossil diesel at constant injection and constant ignition timing. In Fig. 7a, it can be seen that at both timings, addition of FAME to the reference fossil diesel at levels up to 20% v/v resulted in a decrease in CO emission, and that of the unblended methyl esters, DPME emitted the highest levels of CO, while RME emitted the lowest levels of CO. Notwithstanding the range of error present in Fig. 7b, it can be seen that THC emissions from unblended RME and SME are approximately twice those of the other fuels tested, including unblended DPME. Exhaust emissions of CO arise from partial fuel oxidation where either temperatures or the availability of oxygen are insufficient for complete combustion [68], and so it is cautiously suggested that the higher CO levels emitted by DPME relative to both RME and SME (Fig. 7a) may also be attributable to the posited lower adiabatic flame temperature of the former. It is also tentatively suggested that the higher densities and kinematic viscosities of the RME and SME relative to DPME (Table 4), may have resulted in an increased incidence of fuel impingement on the piston bowl and cylinder [56,69], impeding the mixing with air of this fuel fraction and giving rise to the elevated THC emissions of the unblended RME and SME relative to those of DPME (Fig. 7b).

3.4. Particulate mass and number emissions

Fig. 8 shows the total particulate mass emitted by the methyl esters, methyl ester and reference diesel blends, Oman diesel and reference fossil diesel at both constant injection and constant ignition timing. Despite the significant range of measurement variability indicated by the error bars present from repeat measurements of the reference fossil diesel (0% FAME content), it can be seen that the lowest levels of PM were emitted by unblended DPME and RME at both injection timings (Fig. 8). This is consistent with many previous studies of biodiesels and single fatty acid methyl esters where reductions in PM relative to fossil diesel have been observed [30,51,53,70]. Notwithstanding the large degree of test to test variability visible in Fig. 8, the suggested higher PM emissions of the Oman diesel relative to the reference fossil diesel (Fig. 8) can tentatively be attributed to a number of fuel properties, including a shorter duration of ignition delay (Fig. 3) resulting in a longer diffusion control combustion phase [54], a significantly higher sulphur content [71,72], and higher viscosity (which can be expected to increase the extent of fuel rich areas of the in-cylinder charge suitable for soot formation [73]) of the former (Table 4).

Fig. 9a and b show the particle number size distribution of particulates emitted by the methyl esters, methyl ester and reference diesel blends, Oman diesel and reference fossil diesel at both constant injection and constant ignition timing. All fuels tested display a biomodal distribution of particle diameters, with the highest number of particles emitted at a diameter of approximately 20 nm (Fig. 9a and b). However, it is interesting to note that the number of particles emitted of diameter greater than 100 nm decreases more rapidly in the case of unblended DPME, at both timing conditions, relative to all other fuels tested (Fig. 9a and b).

4. Conclusions

From tests of date pit methyl esters in a modern direct injection diesel engine, the following conclusions regarding the combustion and emissions performance of this biodiesel relative to those comprised of rapeseed methyl esters and soybean methyl esters can be drawn:
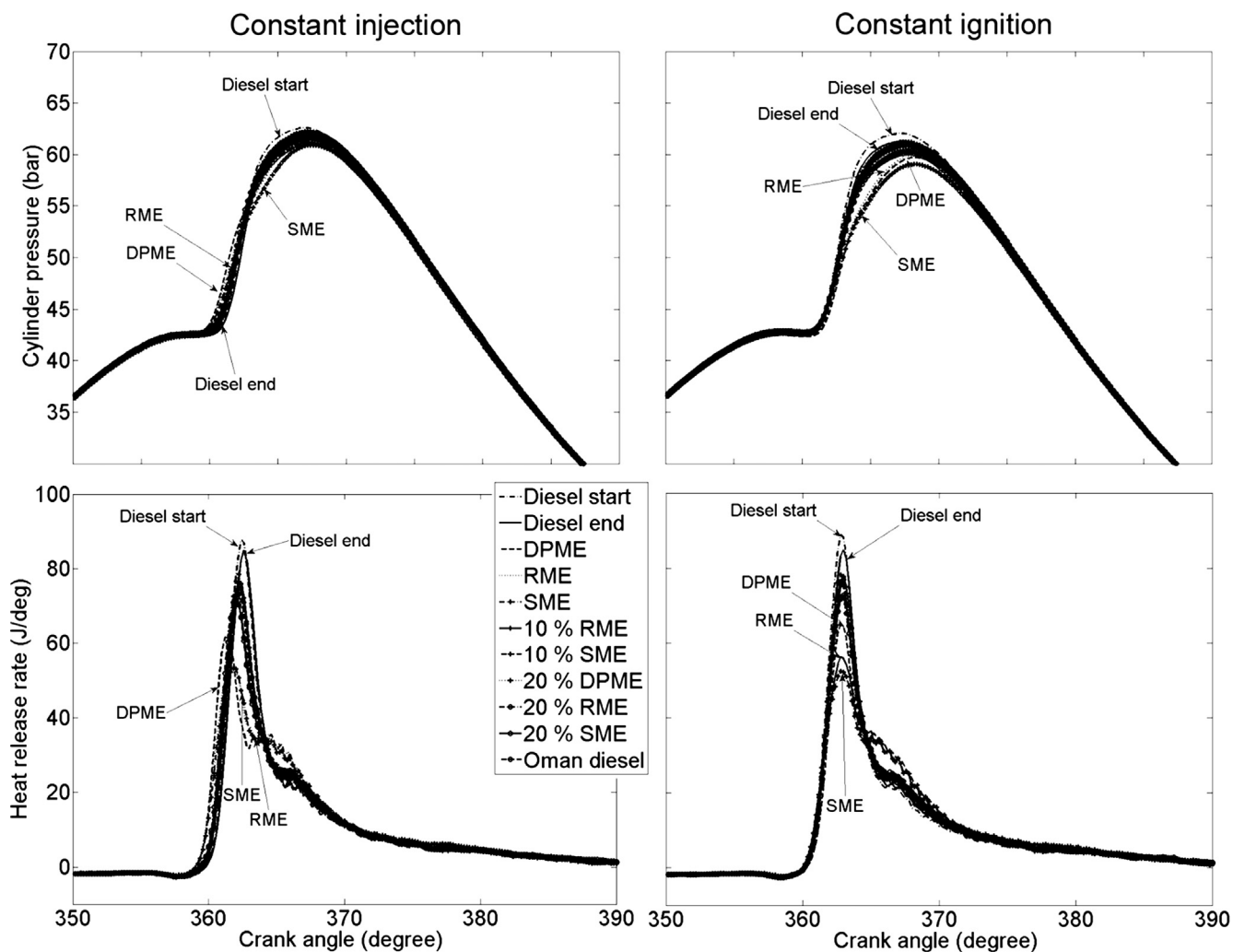
Constant injection

Constant ignition

Fig. 2. In-cylinder pressures and apparent net heat release rates of the methyl esters, methyl ester and reference diesel blends, Oman diesel and reference fossil diesel at constant injection and constant ignition timing.
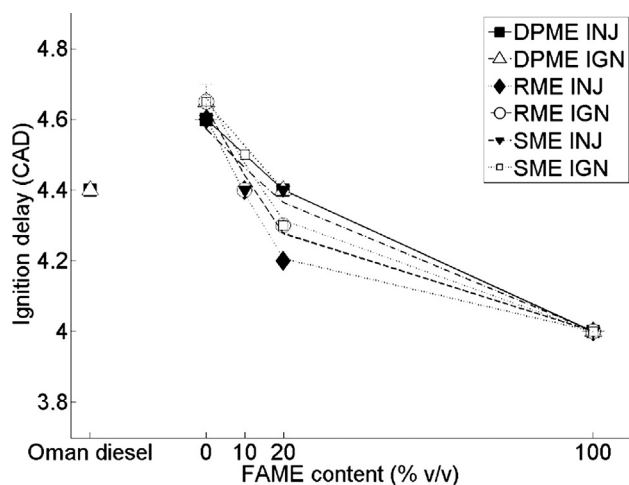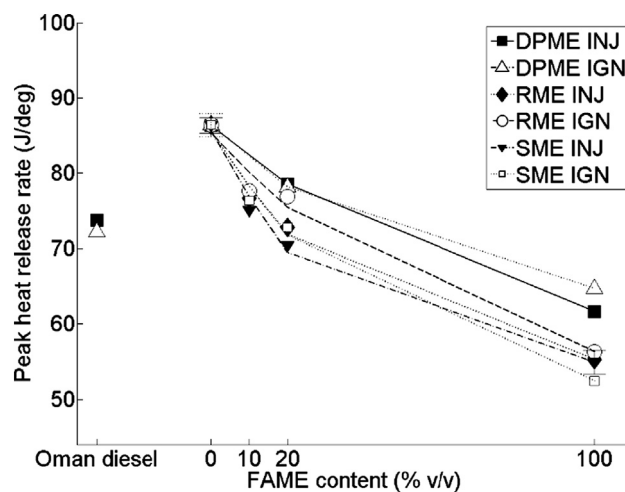

Fig. 3. Ignition delay (SOI to SOC) of the methyl esters, methyl ester and reference diesel blends, Oman diesel and reference fossil diesel at constant injection and constant ignition timing.

Fig. 4. Peak apparent heat release rate of the methyl esters, methyl ester and reference diesel blends, Oman diesel and reference fossil diesel at constant injection and constant ignition timing.

1. DPME displayed a similar duration of ignition delay as RME and SME, both as un-blended methyl esters and as 20% v/v blends with a reference fossil diesel, despite a higher cetane number of the former. While the shorter mean alkyl moiety of DPME relative to RME and

SME might have been expected to result in a longer ignition delay, this was countered by the lower mean number of double bonds present in the date pit methyl esters.
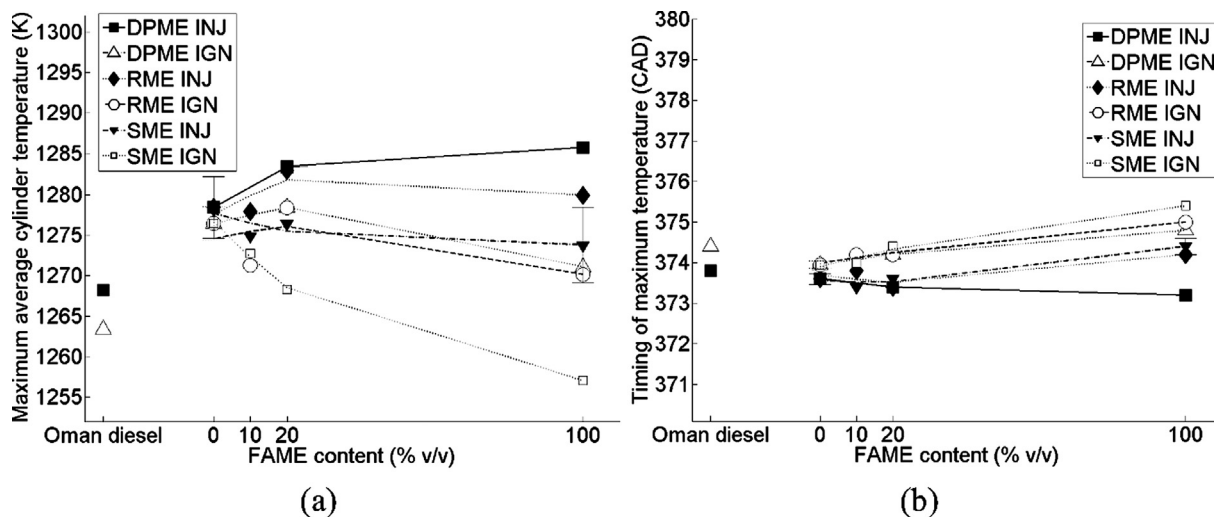
Fig. 5. (a) Calculated maximum in-cylinder global temperature and (b) time of occurrence of maximum global temperature of the methyl esters, methyl ester and reference diesel blends, Oman diesel and reference fossil diesel at constant injection and constant ignition timing.
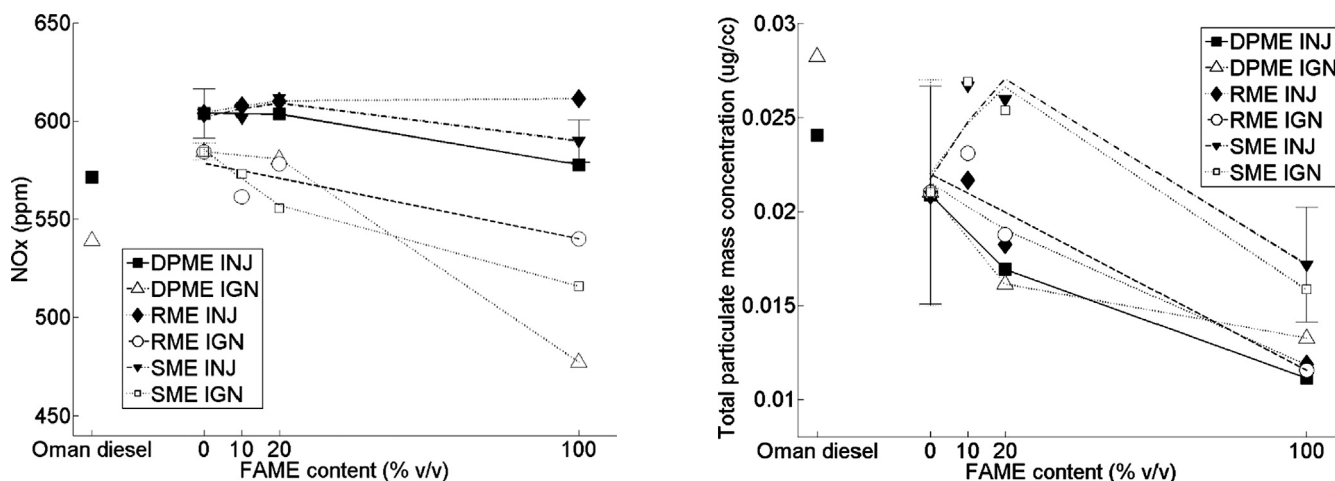

Fig. 6. NOx emissions of the methyl esters, methyl ester and reference diesel blends, Oman diesel and reference fossil diesel at constant injection and constant ignition timing.
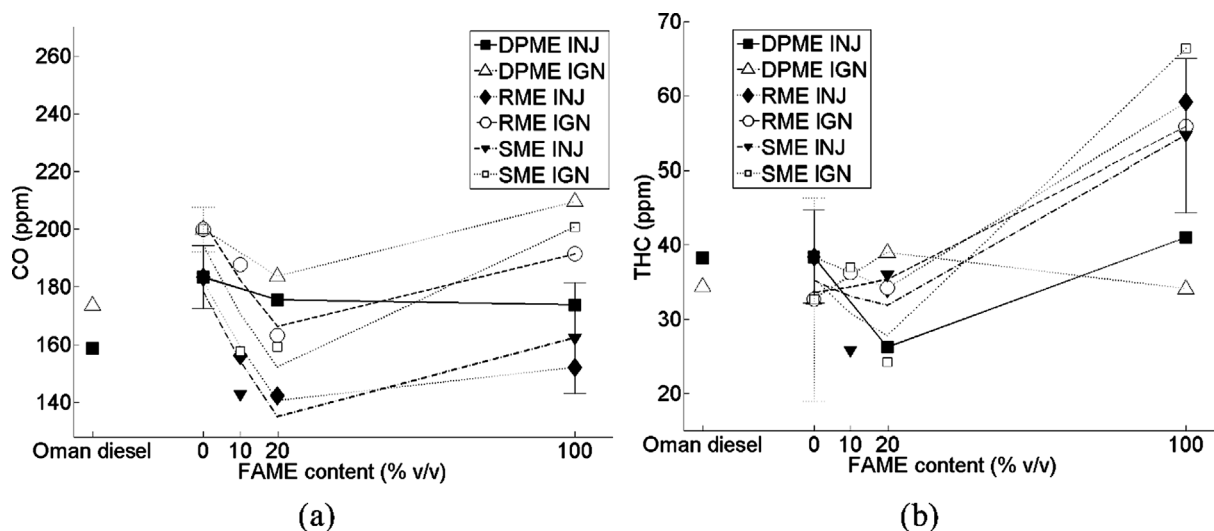

Fig. 8. Total particulate mass emitted by the methyl esters, methyl ester and reference diesel blends, Oman diesel and reference fossil diesel at constant injection and constant ignition timing.

Fig. 7. (a) CO and (b) THC emissions of the methyl esters, methyl ester and reference diesel blends, Oman diesel and reference fossil diesel at constant injection and constant ignition timing.
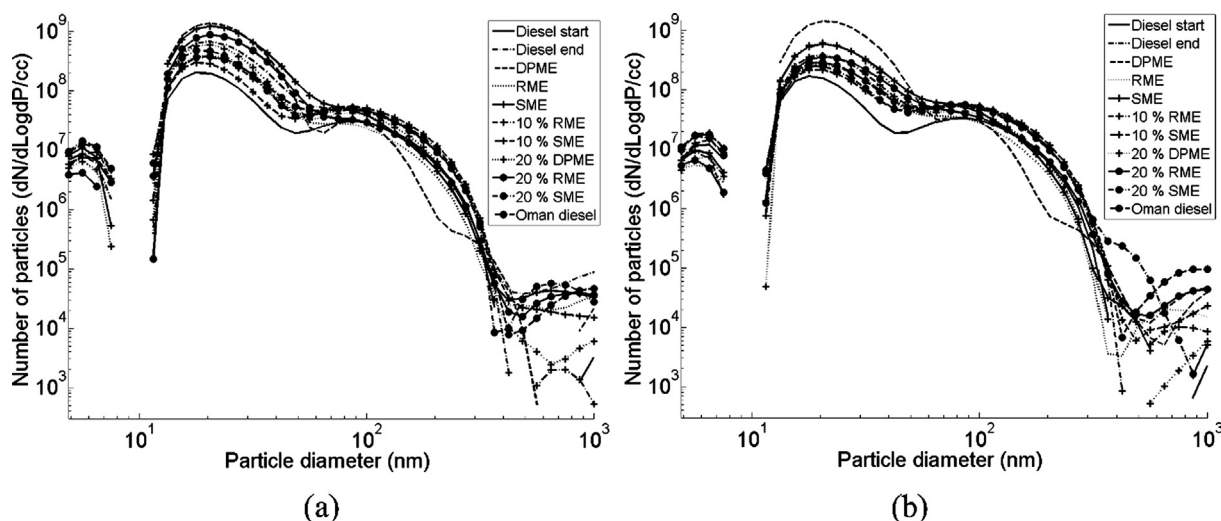
Fig. 9. Particulate emissions of by the methyl esters, methyl ester and reference diesel blends, Oman diesel and reference fossil diesel at (a) constant injection and (b) constant ignition timing.

2. Higher peak heat release rates were exhibited by DPME than either RME or SME, with a faster increase in heat release rates following start of combustion. This higher reactivity of DPME relative to RME and SME is in agreement with the cetane numbers of the methyl esters where an impact on the duration of ignition delay, and thus time available for fuel and air premixing, is not readily apparent.

3. At both constant injection and constant ignition timings, the lowest levels of NOx were emitted by unblended DPME. This is contrary to the higher peak heat release rates and in-cylinder maximum global temperatures of the DPME relative to RME and SME which might have been expected to increase rates of thermal NOx production. However, the shorter mean alkyl moiety chain length and lower mean number of double bonds of the DPME relative to the other esters may have actually resulted in a lower adiabatic flame temperature, and thus lower local temperatures and reduced rates of NOx production.

4. CO and THC emissions were highest in the case of the unblended DPME and RME at constant ignition timing respectively, and potentially attributable to the lower local temperatures suggested by the low levels of NOx emitted by DPME and the higher viscosity of RME.

5. Levels of exhaust particulate matter were lower for the unblended methyl esters than either the reference fossil diesel or the methyl ester and reference diesel blends. No impact of the relative differences in fatty acid ester composition could be seen in the total particulate mass emitted, however, particle number emissions were lower in the range of 100 nm to 200 nm in the case of the unblended DMPE relative to all other fuels tested.

Acknowledgements

References

[1] Gosling SN, Arnell NW. A global assessment of the impact of climate change on water scarcity. Clim Change 2016;134:371–85.
[2] Zecca A, Chiari L. Fossil-fuel constraints on global warming. Energy Policy 2010;38:1–3.
[3] McGlade C, Ekins P. The geographical distribution of fossil fuels unused when limiting global warming to 2 °C. Nature 2015;517:187–90.
[4] Sarlioglu B, Morris CT, Han D, Li S. Driving toward accessibility: a review of technological improvements for electric machines, power electronics, and batteries for electric and hybrid vehicles. IEEE Ind Appl Mag 2017;23:14–25.
[5] Hofmann J, Guan D, Chalvatzis K, Huo H. Assessment of electrical vehicles as a successful driver for reducing CO2 emissions in China. Appl Energy 2016;184:995–1003.
[6] Ellingsen LA-W, et al. The size and range effect: lifecycle greenhouse gas emissions of electric vehicles. Environ Res Lett 2016;11:054010.
[7] Sen B, Ercan T, Tatari O. Does a battery-electric truck make a difference? – Life cycle emissions, costs, and externality analysis of alternative fuel-powered Class 8 heavy-duty trucks in the United States. J Clean Prod 2017;141:110–21.
[8] Turner MC, et al. Long-term ozone exposure and mortality in a large prospective study. Am J Respir Crit Care Med 2016;193:1134–42.
[9] Wang T, Jerrett M, Sinsheimer P, Zhu Y. Estimating PM2.5-associated mortality increase in California due to the Volkswagen emission control defeat device. Atmos Environ 2016;144:168–74.
[10] European Commission & European Parliament and Council. Directive 2009/28/EC of the European Parliament and of the Council of 23 April 2009 on the promotion of the use of energy from renewable sources. Off. J. Eur. Union; 2009. p. 16–62.
[11] US EPA. Renewable Fuel Standard (RFS). Fuels and Fuel Additives (2005). Available at: http://www.epa.gov/otaq/fuels/renewablefuels/index.htm.
[12] Yang H, Zhou Y, Liu J. Land and water requirements of biofuel and implications for food supply and the environment in China. Energy Policy 2009;37:1876–85.
[13] The European Parliament and The Council of the European Union. Directive (EU) 2015/1513 of the European parliament and of the council. (European Commission, 2015).
[14] European Biodiesel Board. 2009-2010: EU biodiesel industry restrained growth in challenging times; 2010.
[15] Cruz JM, Ogunlowo AS, Chancellor WJ, Goss JR. Vegetable oils as fuels for diesel engines. Resour Conserv 1981;6:69–74.
[16] Pryde EH. Vegetable oils as diesel fuels: overview. J Am Oil Chem Soc 1983;60:1557–8.
[17] Ryan TW, Dodge LG, Callahan TJ. The effects of vegetable oil properties on injection and combustion in two different diesel engines. J Am Oil Chem Soc 1984;61:1610–9.
[18] Harrington KJ. Chemical and physical properties of vegetable oil esters and their effect on diesel fuel performance. Biomass 1986;9:1–17.
[19] Graboski MS, McCormick RL. Combustion of fat and vegetable oil derived fuels in diesel engines. Prog Energy Combust Sci 1998;24:125–64.
[20] Basha SA, Gopal KR, Jebaraj S. A review on biodiesel production, combustion, emissions and performance. Renew Sustain Energy Rev 2009;13:1628–34.
[21] Szybist JP, Song J, Alam M, Boehman AL. Biodiesel combustion, emissions and emission control. Fuel Process Technol 2007;88:679–91.
[22] Hoekman SK, Robbins C. Review of the effects of biodiesel on NOx emissions. Fuel Process Technol 2012;96:237–49.
[23] Atadashi IM, Aroua MK, Aziz AA. High quality biodiesel and its diesel engine application: a review. Renew Sustain Energy Rev 2010;14:1999–2008.
[24] Lapuerta M, Armas O, Rodriguezfernandez J. Effect of biodiesel fuels on diesel engine emissions. Prog Energy Combust Sci 2008;34:198–223.
[25] Hoekman SK, Broch A, Robbins C, Ceniceros E, Natarajan M. Review of biodiesel composition, properties, and specifications. Renew Sustain Energy Rev 2012;16:143–69.
[26] Hellier P, Ladommatos N. The influence of biodiesel composition on compression ignition combustion and emissions. Proc Inst Mech Eng Part A J Power Energy 2015;229:714–26.
[27] No S-Y. Inedible vegetable oils and their derivatives for alternative diesel fuels in CI engines: a review. Renew Sustain Energy Rev 2011;15:131–49.
[28] Atabani AE, et al. Non-edible vegetable oils: a critical evaluation of oil extraction, fatty acid compositions, biodiesel production, characteristics, engine performance

and emissions production. Renew Sustain Energy Rev 2013;18:211–45.

[29] Achten WMJ, et al. Jatropha bio-diesel production and use. Biomass Bioenergy 2008;32:1063–84.

[30] Schönborn A, Ladommatos N, Williams J, Allan R, Rogerson J. The influence of molecular structure of fatty acid monoalkyl esters on diesel combustion. Combust Flame 2009;156:1396–412.

[31] Oo CW, et al. Ignition and combustion characteristics of various biodiesel fuels (BDFs). Fuel 2015;158:279–87.

[32] Achten WMJ, et al. Life cycle assessment of Jatropha biodiesel as transportation fuel in rural India. Appl Energy 2010;87:3652–60.

[33] Hou J, Zhang P, Yuan X, Zheng Y. Life cycle assessment of biodiesel from soybean, jatropha and microalgae in China conditions. Renew Sustain Energy Rev 2011;15:5081–91.

[34] Xue J. Combustion characteristics, engine performances and emissions of waste edible oil biodiesel in diesel engine. Renew Sustain Energy Rev 2013;23:350–65.

[35] Lapuerta M, Herreros JM, Lyons LL, García-Contreras R, Briceño Y. Effect of the alcohol type used in the production of waste cooking oil biodiesel on diesel performance and emissions. Fuel 2008;87:3161–9.

[36] Ozsezen, A. N., Canakci, M. & Sayin, C. Effects of Biodiesel from Used Frying Palm Oil on the Performance, Injection, and Combustion Characteristics of an Indirect Injection Diesel Engine. http://dx.doi.org/10.1021/ef700447z.

[37] Lin Y-S, Lin H-P. Study on the spray characteristics of methyl esters from waste cooking oil at elevated temperature. Renew. Energy 2010;35:1900–7.

[38] Leung DYC, Guo Y. Transesterification of neat and used frying oil: optimization for biodiesel production. Fuel Process Technol 2006;87:883–90.

[39] Canakci M, Sanli H. Biodiesel production from various feedstocks and their effects on the fuel properties. J Ind Microbiol Biotechnol 2008;35:431–41.

[40] Wu F, Wang J, Chen W, Shuai S. A study on emission performance of a diesel engine fueled with five typical methyl ester biodiesels. Atmos Environ 2009;43:1481–5.

[41] Jenkins RW, Stageman NE, Fortune CM, Chuck CJ. Effect of the type of bean, processing, and geographical location on the biodiesel produced from waste coffee grounds. Energy Fuels 2014;28:1166–74.

[42] Kwon EE, Yi H, Jeon YJ. Sequential co-production of biodiesel and bioethanol with spent coffee grounds. Bioresour Technol 2013;136:475–80.

[43] Al-Hamamre Z, et al. Oil extracted from spent coffee grounds as a renewable source for fatty acid methyl ester manufacturing. Fuel 2012;96:70–6.

[44] Chapagain BP, Yehoshua Y, Wiesman Z. Desert date (Balanites aegyptiaca) as an arid lands sustainable bioresource for biodiesel. Bioresour Technol 2009;100:1221–6.

[45] Nehdi I, Omri S, Khalil MI, Al-Resayes SI. Characteristics and chemical composition of date palm (Phoenix canariensis) seeds and seed oil. Ind Crops Prod 2010;32:360–5.

[46] Jamil F, et al. Optimization of oil extraction from waste "Date pits" for biodiesel production. Energy Convers Manage 2016;117:264–72.

[47] Azeem MW, et al. Production of biodiesel from low priced, renewable and abundant date seed oil. Renew. Energy 2016;86:124–32.

[48] Al-Zuhair S, et al. Biodiesel production from oils extracted from date pits. Green Sustain Chem 2017;7:48–56.

[49] Essa MM, Manickavasagan A, Sukumar E. Dates: Production, Processing, Food, and Medicinal Values. CRC Press; 2012.

[50] Mabood F, et al. Determination of sucrose in date fruits (Phoenix dactylifera L.) growing in the Sultanate of Oman by NIR spectroscopy and multivariate calibration. Spectrochim Acta Part A Mol Biomol Spectrosc 2015;150:170–4.

[51] Pinzi S, Rounce P, Herreros JM, Tsolakis A, Pilar Dorado M. The effect of biodiesel fatty acid composition on combustion and diesel engine exhaust emissions. Fuel 2013;104:170–82.

[52] Benjumea P, Agudelo JR, Agudelo AF. Effect of the degree of unsaturation of biodiesel fuels on engine performance, combustion characteristics, and emissions.

Energy Fuels 2011;25:77–85.

[53] Zhu L, Cheung CS, Huang Z. Impact of chemical structure of individual fatty acid esters on combustion and emission characteristics of diesel engine. Energy 2016;107:305–20.

[54] Hellier P, Ladommatos N, Allan R, Payne M, Rogerson J. The impact of saturated and unsaturated fuel molecules on diesel combustion and exhaust emissions. SAE Int J Fuels Lubr 2011;5:106–22.

[55] Hellier P, Ladommatos N, Allan R, Rogerson J. The influence of fatty acid ester alcohol moiety molecular structure on diesel combustion and emissions. Energy Fuels 2012;26:1912–27.

[56] Hellier P, Ladommatos N, Yusaf T. The influence of straight vegetable oil fatty acid composition on compression ignition combustion and emissions. Fuel 2015;143:131–43.

[57] Energy Institute (formerly Institute of Petroleum). IP 12: Determination of specific energy (ASTM D240–09). 2001.

[58] Ramos MJ, Fernández CM, Casas A, Rodríguez L, Pérez Á. Influence of fatty acid composition of raw materials on biodiesel properties. Bioresour Technol 2009;100:261–8.

[59] Wang L, Yu H, He X, Liu R. Influence of fatty acid composition of woody biodiesel plants on the fuel properties. J Fuel Chem Technol 2012;40:397–404.

[60] Peirce DM, Alozie NSI, Hatherill DW, Ganippa LC. Premixed burn fraction: its relation to the variation in NOx emissions between petro- and biodiesel. Energy Fuels 2013;27:3838–52.

[61] Westbrook CK. Chemical kinetics of hydrocarbon ignition in practical combustion systems. Proc Combust Inst 2000;28:1563–77.

[62] Mehl M, et al. Autoignition behavior of unsaturated hydrocarbons in the low and high temperature regions. Proc Combust Inst 2011;33:201–8.

[63] Nerva J-G, Genzale CL, Kook S, Garcia-Oliver JM, Pickett LM. Fundamental spray and combustion measurements of soy methyl-ester biodiesel. Int J Engine Res 2012;14:373–90.

[64] Menkiel B, Donkerbroek A, Uitz R, Cracknell R, Ganippa L. Combustion and soot processes of diesel and rapeseed methyl ester in an optical diesel engine. Fuel 2014;118:406–15.

[65] Ickes AM, Bohac SV, Assanis DN. Effect of fuel cetane number on a premixed diesel combustion mode. Int J Engine Res 2009;10:251–63.

[66] Szybist JP, Boehman AL, Taylor JD, McCormick RL. Evaluation of formulation strategies to eliminate the biodiesel NOx effect. Fuel Process Technol 2005;86:1109–26.

[67] Mueller CJ, Boehman AL, Martin GC. An experimental investigation of the origin of increased NOx emissions when fueling a heavy-duty compression-ignition engine with soy biodiesel. SAE Tech. Pap. Ser. 2009. p. 1792–2009.

[68] Heywood JB. Internal combustion engine fundamentals. McGrawHill Series in Mechanical Engineering. McGraw-Hill Book Company; 1988.

[69] Chen P-C, Wang W-C, Roberts WL, Fang T. Spray and atomization of diesel fuel and its alternatives from a single-hole injector using a common rail fuel injection system. Fuel 2013;103:850–61.

[70] Shahir VK, Jawahar CP, Suresh PR. Comparative study of diesel and biodiesel on CI engine with emphasis to emissions—a review. Renew Sustain Energy Rev 2015;45:686–97.

[71] Zhu R, Cheung CS, Huang Z, Wang X. Regulated and unregulated emissions from a diesel engine fueled with diesel fuel blended with diethyl adipate. Atmos Environ 2011;45:2174–81.

[72] Maricq MM, Chase RE, Xu N, Laing PM. The effects of the catalytic converter and fuel sulfur level on motor vehicle particulate matter emissions: light duty diesel vehicles. Environ Sci Technol 2002;36:283–9.

[73] Tree DR, Svensson KI. Soot processes in compression ignition engines. Prog Energy Combust Sci 2007;33:272–309.